Rotationally Resolved C-2 Symmetric Conformers of Bis-(4-hydroxyphenyl)methane: Prototypical Examples of Excitonic Coupling in the S-1 and S-2 Electronic States

ARTICLE *in* THE JOURNAL OF PHYSICAL CHEMISTRY A · JUNE 2011

Impact Factor: 2.69 · DOI: 10.1021/jp200804t · Source: PubMed

THE JOURNAL OF PHYSICAL CHEMISTRY A

ARTICLE

pubs.acs.org/JPCA

Rotationally Resolved C_2 Symmetric Conformers of Bis-(4-hydroxyphenyl)methane: Prototypical Examples of Excitonic Coupling in the S_1 and S_2 Electronic States

Shin Grace Chou,[†] Chirantha P. Rodrigo,[‡] Christian W. Müller,[‡] Kevin O. Douglass,[†] Timothy S. Zwier,[*,‡] and David F. Plusquellic[*,†]

[†]Biophysics Group, Optical Technology Division, Physical Measurement Laboratory, National Institute of Standards and Technology, Gaithersburg, Maryland 20899-8441, United States

[‡]Department of Chemistry, Purdue University, West Lafayette, Indiana 47907, United States

Supporting Information

ABSTRACT: Rotationally resolved microwave and ultraviolet spectra of jet-cooled bis-(4-hydroxyphenyl)methane (b4HPM) have been obtained using Fourier-transform microwave and UV laser/molecular beam spectrometers. A recent vibronic level study of *b*4HPM [Rodrigo, C. P.; Müller, C. W.; Pillsbury, N. R.; James, W. H., III; Plusquellic, D. F.; Zwier, T. S. *J. Chem. Phys.* **2011**, *134*, 164312] has assigned two conformers distinguished by the orientation of the in-plane OH groups and has identified two excitonic origins in each conformer. In the present study, the rotationally resolved bands of all four states have been well-fit to asymmetric rotor Hamiltonians. For the lower exciton (S_1) levels, the transition dipole moment (TDM) orientations are perpendicular to the C_2 symmetry axes and consist of 41(2):59(2) and 34(2):66(2)% *a*:*c* hybrid-type character. The S_1 levels are therefore delocalized states of B symmetry and represent the antisymmetric combinations of the zero-order locally excited states of the *p*-cresol-like chromophores. The TDM polarizations of bands located at ≈132 cm^{-1} above the S_1 origins are exclusively *b*-type and identify them as the upper exciton S_2 origin levels of A symmetry. The TDM orientations and the relative band strengths from the vibronic study have been analyzed within a dipole−dipole coupling model in terms of the localized TDM orientations, μ_{loc}, on the two chromophores. The out-of-the-ring plane angles of μ_{loc} are both near 20° and are similar to results for diphenylmethane [Stearns, J. A.; Pillsbury, N. R.; Douglass, K. O.; Müller, C. W.; Zwier, T. S.; Plusquellic, D. F. *J. Chem. Phys.* **2008**, *129*, 224305]. The in-plane angles are, however, rotated by 14 and 18° relative to DPM and, in part, explain the smaller than expected exciton splittings of these two conformers.

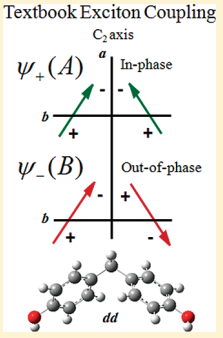

I. INTRODUCTION

The physical models of excitonic interactions in bichromophores have served as a basis for understanding a number of photophysical processes in organic crystals and molecular aggregates that are commonly used in organic light emitting diodes and thin film organic solar cells.[1−5] Fundamental insight into these models has come from state-resolved studies of model systems isolated in the gas phase where a detailed view of intrinsic properties associated with a small number of exciton coupled states are possible. Such properties include the extent of delocalization and polarization of the coupled states, the geometric factors that impact the state symmetry, the order and exciton splitting, and the vibronic-induced mechanisms associated with exciton state mixing and quenching. In particular, the importance of vibronic coupling in exciton coupled bichromophores has come under close scrutiny in the past several years.[6−9] Excitonic coupling in the hydrogen bonded dimer of 2-aminopyridine[6,7,10] has been investigated in detail using the vibronic coupling theory first developed by Fulton and Goutermann[11,12] to describe excitonic interactions of molecular dimers in crystals. This original theory was extended to include the intermolecular modes to explain the transitions observed in the low frequency region and the small excitonic splitting between the electronically forbidden S_1 and fully allowed S_2 origins.[10]

Diphenylmethane (DPM) has also served as a model system of excitonic coupling in symmetric bichromophores. Both crystalline[13] and gas phase[14,15] results have been reported on the S_1 and S_2 states split by only ≈120 cm^{-1}. Under jet-cooled conditions, dispersed fluorescence results[14] have revealed clear signatures of vibronic coupling of S_1 torsional modes in the vicinity of the S_2 origin. In a high resolution study,[15] the rotational structure of the S_1 origin was fully analyzed, although rotational perturbations of the S_2 origin prevented a similar analysis of the upper exciton level. Nevertheless, application of a simple model of the excitonic interactions between the two toluene-like chromophores

Special Issue: David W. Pratt Festschrift

Received: January 25, 2011
Revised: May 5, 2011
Published: June 03, 2011

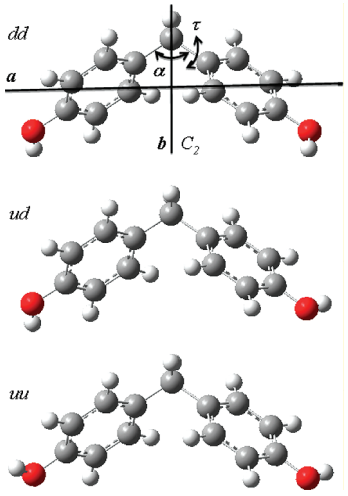

Figure 1. Structures of the three conformers of b4HPM in the principal axis frames. For the *dd* conformer, the three "soft" degrees of freedom associated with the lowest frequency modes are shown and include the two torsional coordinates, τ_1 and τ_2, defined as the dihedral angle between the planes formed by Ph−CH_2−Ph and the three ring carbon atoms nearest to the methylene group and the Ph−CH_2−Ph bending (butterfly) coordinate, α.

was used to explain the observed transition dipole moment (TDM) orientations in terms of localized TDMs.

In this study, we report on the rotationally resolved UV spectra of a similar bichromophore, bis-(4-hydroxyphenyl)methane (b4HPM) that differs from DPM by the addition of two OH groups in the *para* position. As illustrated in Figure 1, three possible conformational isomers are distinguished by the up−up (*uu*), down−down (*dd*), or *ud*/*du* orientations of the two in-plane OH groups. The ab initio ground state surface shown in Figure 2 illustrates the interconversion pathways for these conformers along the torsional coordinates, τ_1 and τ_2. In the jet-cooled vibronic part of this study,[16] results from UV−UV holeburning spectra have identified two independent conformers, labeled A and B, having nearly identical excitation spectra separated by 25 cm^{-1}. Furthermore, similar to DPM, both conformers were found to have an exciton splitting of 132 cm^{-1}, which is quite small compared to many other bichromophores. In the present work, the rotationally resolved spectra of the S_0-S_1 and S_0-S_2 origin transitions of both conformers are fully assigned. The observed TDM orientations present classic examples of strong excitonic coupling between two identical chromophores positioned in C_2 symmetric structures. From the analysis of the structural and the TDM data for b4HPM, the impact of the conformation and the chromophore strength on the excitonic interactions are examined within the dipole−dipole coupling model and the finding are compared with results from a similar analysis previously reported for DPM.[14]

II. EXPERIMENTAL METHODS

Rotationally resolved fluorescence excitation spectra of b4HPM were measured using a UV laser/molecular beam spectrometer discussed elsewhere.[17] Briefly, an Ar^+-pumped (488 nm line) cw ring dye laser using Rhodamine 590 generated ≈500 mW of narrow band light (≈1 MHz) near 568 nm. Approximately 10 mW of the UV light at 284 nm was generated in an external resonant cavity containing a β-barium borate crystal. b4HPM was heated to 423 K (150 °C) in a three-chamber quartz source. Typically, the

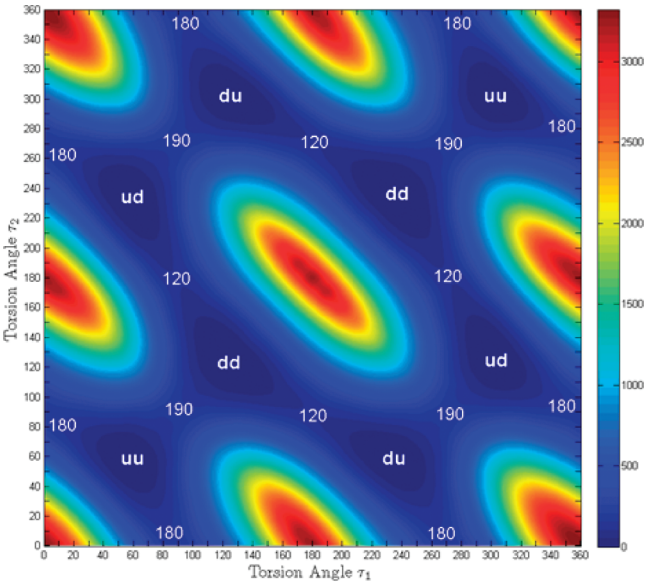

Figure 2. Ground state torsional potential energy surface for b4HPM calculated at the B3LYP/6-311G** level of theory. The axes represent the torsion angles of the *p*-cresol rings, τ_1 and τ_2 for transformation between the different conformational isomers. The calculated barrier heights in cm^{-1} are given in the figure.

vapor was mixed with 21−29 kPa (160−200 Torr) of Ar gas and expanded into a source chamber through a 125 μm nozzle. The molecular beam was skimmed and crossed at right angles with a slightly focused UV beam 18 cm downstream of the source. Laser-induced fluorescence at the beam crossing was collected with 20% efficiency using two spherical mirrors[18] and detected using a photomultiplier and computer interfaced photon counter. The Doppler limited resolution of the spectrometer is 18(1) MHz at 330 nm[19] and is therefore expected to be 21(1) MHz at 284 nm. Relative frequency calibration was performed using a HeNe stabilized reference cavity[17,20] and absolute frequencies were obtained using a wavemeter accurate to ±0.02 cm^{-1}. b4HPM was available commercially and used at the stated purity of >95%.

The pure rotational spectrum of b4HPM was recorded in a mini-Fourier transform microwave (MW) spectrometer[21,22] operating between 11 and 18 GHz. Samples were loaded into a heated reservoir nozzle and heated to 433 K (160 °C) and expanded at 101 kPa (760 Torr) with an 80% He/20% Ne gas mixture. The ground state rotational constants determined from the UV fits were used to target specific MW measurements of both conformers to improve the accuracy of parameters obtained from the least-squares fits.

All spectra were fit to an asymmetric rotor Hamiltonian (representation I^r) using a distributed parallel version of the genetic algorithm (GA) program[23,24] beginning with ground state rotational constants estimated from ab initio theory. Parameter uncertainties from linear least-squares fits of the bands were confirmed from comparisons with results from repeated GA runs on the same band and from independent spectra taken several weeks to months apart.

III. RESULTS AND ANALYSIS

A. Ground States and S_1 and S_2 Origin Bands of the A and B Conformers. Based on the vibronic data,[16] the MW spectrum

Table 1. Rotational Constants of the Two Conformers of b4HPM from Linear Least Squares Fits of the FTMW Spectrum[a]

	conf. A		conf. B	
S_0	expt.	MP2 (*dd*)	expt.	MP2 (*uu*)
A'' MHz	1569.7774(2) [b]	1526.63	1571.899(1)	1516.91
B'' MHz	261.156(2)	267.37	261.211(4)	267.90
C'' MHz	250.150(2)	255.80	249.958(5)	256.66
$\Delta I''$ u·Å^2	−236.80(2)	−245.55	−234.41(5)	−250.55
Δ_J MHz	$2.20(3) \times 10^{-5}$	1.65×10^{-5}	$4.59(8) \times 10^{-5}$	1.65×10^{-5}
Δ_{JK} MHz	$-2.21(1) \times 10^{-4}$	1.07×10^{-3}	$-3.79(9) \times 10^{-4}$	1.05×10^{-3}
Δ_K/MHz	$3.279(6) \times 10^{-3}$	2.53×10^{-3}	$3.39(2) \times 10^{-3}$	2.82×10^{-3}
δ_J MHz [c]		5.01×10^{-6}		5.06×10^{-6}
δ_k MHz [c]		-2.55×10^{-3}	$8.9(6) \times 10^{-4}$	-1.21×10^{-3}
band type %	100 *b*	100 *b*	100 *b*	100 *b*
assigned	28		17	
σ kHz	1.9		2.5	

[a] The predicted parameters from MP2/cc-pVTZ calculations are also given. [b] Uncertainties shown in parentheses refer to the last digits shown and are Type A, coverage factor $k = 1$ (1 std. dev.; ref 25). [c] Asymmetric reduction used.

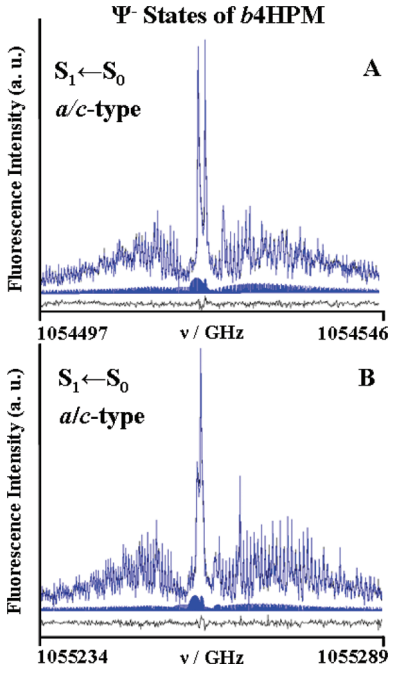

Figure 3. Rotationally resolved spectra of the $S_1 \leftarrow S_0$ origin regions of conformers A (upper) and B (lower) of b4HPM. The simulated spectra are superimposed and the stick spectra and residuals are shown below each. The pure *a*/*c*-type hybrid bands indicate completely delocalized wave functions having the Ψ^- exciton levels at lowest energy.

of b4HPM is expected to contain contributions from two independent conformers. Beginning with ground state predictions from the UV fits, 28 *b*-type rotational lines were assigned to conformer A and 17 *b*-type lines were assigned to conformer B. The rotational constants obtained from the fits of these two bands are given in Table 1. In both cases, Watson centrifugal distortion constants were required to reduce the differences between the observed minus calculated frequencies to within the estimated measurement uncertainty of ±2 kHz (Type B, $k = 1$).[25] The MW spectrum and assignments are given in the Supporting Information.

From Table 1, the observed differences in rotational constants of conformers A and B are less than 0.2%, indicating the structural differences are small, as might be expected for the different OH group orientations of these two conformers.[26] The observation of only *b*-type lines indicates both conformers possess a net dipole moment oriented along the *b*-inertial axis. This axis coincides with the C_2 symmetry axes for the *uu* and *dd* conformers. The absence of lines associated with the other band types indicates that both ground state structures have C_2 symmetry.

B. S_1 Origin Bands of the A and B Conformers. In the vibronic study,[16] UV−UV holeburning established the presence of two nearly identical band systems separated by 25 cm^{-1} that correspond to two conformers of b4HPM labeled A and B. The $S_1 \leftarrow S_0$ origins of conformers A and B are located at 35175.00 and 35199.65 cm^{-1}, respectively. Note that these are the vacuum wavelength corrected positions for the transitions. The rotationally resolved spectra of these two bands are shown in the upper and lower panels of Figure 3, respectively. The two prominent features observed in the central part of each spectrum are a result of rotational transition pile-ups that obey *a*- or *c*-type selection rules. For input to the GA fitting procedure, the initial parameter set made use of the band types identified above, the ground state constants obtained from ab initio results and the upper state constants (expressed as changes relative to the ground state) that could account for the overall appearance of these spectra using features of the *JB95* fitting software.[27−29] Other parameters such as rotational temperatures and rotational line width used in the calculations were permitted to vary over reasonable ranges. Full convergence to the experimental data was found after a few iterative refinements of the parameter ranges and final fits were obtained using the average values from ten independent data sets. For the final data set, the ground state constants were fixed to the MW values reported in Table 1. The corresponding simulated spectra are superimposed in Figure 3, and the residuals are shown below each trace to illustrate the quality of the fits.

The parameters and uncertainties were confirmed using the traditional line assignment/linear least-squares approach together with nonlinear least-squares fits of the band types, temperatures, and line widths.[27−29] The best-fit parameters are given in Table 2. For both bands, the S_1-state rotational constants

Table 2. Parameters from Least Squares Fits of the S_1 Spectra of Conformers A and B of b4HPM

S_1 origin	conf. A	conf. B
ΔA MHz	−0.587(2)[a]	+2.849(9)
ΔB MHz	+4.274(1)	+3.605(2)
ΔC MHz	+0.375(1)	+0.047(1)
$\Delta\Delta I$ u·Å^2	+28.01(1)	+26.54(1)
$\Delta\Delta_J$ MHz	$-5.5(3) \times 10^{-6}$	$-7.5(9) \times 10^{-6}$
$\Delta\Delta_{JK}$ MHz	$-1.1(1) \times 10^{-4}$	
$\Delta\Delta_K$ MHz	$-5.2(1) \times 10^{-4}$	$-8.4(5) \times 10^{-4}$
$\Delta\Delta\delta_k$ MHz [b]		$-4.0(2) \times 10^{-3}$
origin/rel. cm^{-1}	35175.00(2)	35199.65(2)/+24.65(2)
band type %	41(2) *a*/59(2) *c*	34(2) *a*/66(2) *c*
$\Delta v_G/\Delta v_L$ MHz	21/50(2)	21/48(2)
T_1/T_2 wt/K [b]	3.0(1)/9(1)/0.33(3)	4.0(5)/11(1)/0.70(5)
$\theta_{a/c}$ °	−0.546(4)	−0.468(3)
assigned	250	350
σ MHz	3.4	2.3

[a] Uncertainties shown in parentheses refer to the last digits shown and are Type A, coverage factor k = 1 (1 std dev; ref 25). [b] Asymmetric reduction used.

change very little (<2%) relative to the ground states, although the small differences between the two conformers are sufficient to alter the general appearance of the bands in Figure 3. In both cases, the TDM orientations reside in the *a*/*c*-principal axis frames (see Figure 1) and are determined from the magnitudes of the *a*- and *c*-type band components. The corresponding TDM angles relative to the *a*-axes are ±51.4(1.2)° and ±54.3(1.2)° for the A and B conformers, respectively. To within the signal-to-noise of the measurements, the small residuals shown in the Figure 3 indicate the contribution of *b*-type character to the rotational band type of both S_1 origins is less than 2%.

The TDM results give direct information about the localized versus delocalized excitation of the S_1 states of b4HPM. For example, it is known that the S_1 TDM orientation of the *p*-cresol monomer[30] is orientated along the *b*-inertial axis which is perpendicular to the axis of the substituents. It is also clear for any of the three conformational structures shown in Figure 1 that the TDM orientation for such a localized excitation on the monomer would have a sizable component along the *b*-inertial axis in b4HPM. Therefore, the complete absence of *b*-type character indicates the excited state geometries retain the C_2 symmetry of the ground state and the two excitonic states represent the delocalized antisymmetric combinations (Ψ^-) of the zeroth-order excited states of the *p*-cresol-like chromophores.

C. S_2 Origin Bands of the A and B Conformers. Dispersed fluorescence results from the vibronic study[16] have identified the upper excitonic S_2 origin of conformer A at 35306.92 cm^{-1}, which is +131.92 cm^{-1} above the S_1 origin. The rotationally resolved spectrum of this band is shown in the upper panel of Figure 4. The change in the electronic state character is immediately apparent from the overall appearance of this band, which lacks the central feature(s) characteristic of *a*- or *c*-type rotational structure, and therefore, the spectrum has the character of a pure *b*-type band. From the TDM analysis of the S_1 state given above, the upper exciton state, Ψ^+, is expected to be the delocalized positive combination of the *p*-cresol-like

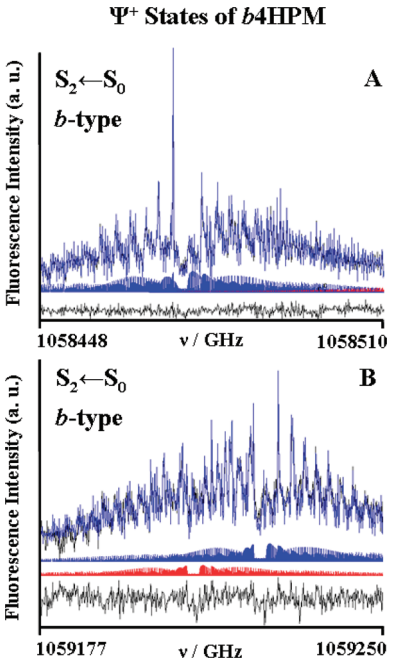

Figure 4. Rotationally resolved spectra of the $S_2 \leftarrow S_0$ origin regions of conformers A (upper) and B (lower) of b4HPM. The simulated spectra are superimposed and the stick spectra and residuals are shown below each. The pure *b*-type bands indicate completely delocalized wave functions having the Ψ^+ exciton levels at highest energy. For conformer A, a vibronic band of S_1 begins to appear on blue edge of the S_2 origin (S_2 + 2.2640 cm^{-1}).

excitations. Therefore, the TDM for Ψ^+ is expected to have an orientation along the C_2 symmetry axis, which is the *b*-inertial axis. This is consistent with our experimental observation. The final analysis of this band made use of GA fitting program where the ground state constants were held fixed to the MW values reported in Table 1. The band was well-fit to an asymmetric rotor model as evident from the small residuals shown below the spectrum. The best-fit parameters are summarized in Table 3. The most salient difference relative to the S_1 parameters is the large change in the A constant which decreases by more than 24 MHz relative to S_0.

The S_2 origin region of conformer B is also ≈132 cm^{-1} above the corresponding S_1 origin[16] and shown in the lower panel of Figure 4. However, the overall appearance stands in contrast to the S_2 state of conformer A by the lack of a clear *b*-type band gap near the band center. Initial GA predictions that used the S_0 parameters fixed at the MW values located one *b*-type band on the blue side of the spectrum in Figure 4. However, large residuals from this fit still remained. Closer examination of the residuals suggested the presence of a second *b*-type band. Upon including parameters for two independent *b*-type bands in the GA program, the residuals decreased to near the signal-to-noise of the measurements after several iterations. The best-fit parameters of the two bands are given in Table 3. The two bands are split by 0.47355(1) cm^{-1} and have a central position relative to S_1 located at +132.02(2) cm^{-1}. This position is very similar to the excitonic splitting of 131.92(2) cm^{-1} found for conformer A. However, the changes in the rotational constants (especially ΔA) are significantly smaller than the ones observed for conformer A. Attempts to refit this region using changes in the rotational constants similar to those of conformer A were entirely

Table 3. Parameters from Least Squares Fits of the S_2 Spectra of Conformers A and B of b4HPM

S_2 origin	conf. A	conf. B	
ΔA MHz	−24.447(8)[a]	+1.805(29)	−3.868(31)
ΔB MHz	+4.256(4)	+2.525(7)	+2.799(9)
ΔC MHz	+1.953(5)	+0.165(5)	+0.464(11)
$\Delta\Delta I$ u·Å^2	+10.28(1)	+17.56(5)	+15.97(4)
$\Delta\Delta_J$ MHz	$+1.8(2) \times 10^{-5}$	$+3.0(2) \times 10^{-5}$	
$\Delta\Delta_{JK}$ MHz	$-3.9(1) \times 10^{-4}$	$-4.6(3) \times 10^{-4}$	$+9.9(1) \times 10^{-4}$
$\Delta\Delta_K$ MHz	$+7.3(5) \times 10^{-4}$	$+5.9(3) \times 10^{-3}$	$-3.7(2) \times 10^{-3}$
origin/rel. cm^{-1}	35306.92(2)/+131.92(2)	35331.44(2)[b]/+131.79(2)	35331.91(2)[b]/+132.26(2)
band type %	100 *b*	100 *b*	100 *b*
$\Delta\upsilon_G/\Delta\upsilon_L$ MHz [a]	21/53(2)	21/48	21/48
T_1/T_2 wt/K [b]	4.2(2)/13(1)/0.21(1)	3.0/9.0/1.0	3.0/9.0/1.0
assigned	252	109	95
σ MHz	2.3	4.6	3.7

[a] Uncertainties shown in parentheses refer to the last digits shown and are Type A, coverage factor $k = 1$ (1 std dev; ref 25). [b] Separation of bands is 14197(1) MHz or 0.47355(1) cm^{-1}.

unsuccessful. We also note that the exciton state order of both conformers is the same as that reported for DPM.[14,15]

D. S_1 Vibronic Bands of the A and B Conformers. Several vibronic bands were measured to establish their vibronic level symmetry in regions near the S_1 and S_2 origins. The spectra included three torsional mode bands assigned to the S_0-S_1 T_0^1, $\overline{T}_0{}^2$, and $\overline{T}_1{}^1$. Bands of both conformers located to the high frequency side of the S_2 origins by <5 cm^{-1} were also observed and assigned to the symmetric phenyl flap, R_0^1.[16] All of these bands were well-fit to asymmetric rotor models using the GA methods discussed above. The best-fit parameters, spectra, and residuals are shown in the Supporting Information. In every case, pure *a*/*c*-type hybrid bands were observed as expected for totally symmetric vibronic bands of S_1. The TDM orientations further confirm the absence of the third *ud*/*du* conformer, which, because of electronic and structural asymmetry, would likely have character from all three band types.

IV. DISCUSSION

In the classic Textbook example of strong excitonic coupling between two identical chromophores, the localized transition dipole moments (TDM) interact to mix the degenerate electronic states of the monomers and give a pair of delocalized eigenstates, Ψ^+ and Ψ^-. From the rotationally resolved results, the electronic state properties of diphenylmethane (DPM)[15] and the two conformers of b4HPM studied here fit well within this idealized limit. The observed TDM orientations reflect the C_2 symmetry of both the nuclear and delocalized electronic wave functions and identify the lower excitonic state as the minus combination of the localized S_1 states of the monomers, Ψ^-, and the upper component as the plus combination, Ψ^+. However, in DPM, complications to this simple model were reported at the state-resolved level where large rotational level perturbations of the Ψ^+ state remain unexplained[15] and unusual deviations from the propensity rules for vibronic coupling between the S_1 and S_2 states were identified for torsional modes undergoing $\Delta v > \pm 1$ quantum number changes.[14]

The addition of two hydroxy groups in b4HPM has simplified this picture tremendously (but not completely). At the rotational level, both the S_1 and S_2 states of the two conformers are well fit to asymmetric rotor models, and as reported in the vibronic study,[16] the internal mixing between the S_1 and S_2 states is largely explained. In the latter case, a slightly modified treatment of the vibronic coupling formalism[11,12] first applied to the intermolecular modes of the 2-aminopyridine dimer by Leutwyler and coworkers[10] adequately predicts the fluorescence excitation and dispersed emission intensity progressions for two ring mode pairs, $6a/6\overline{a}$ and $1/\overline{1}$ and two inter-ring modes pairs, $T/\overline{T}$, $R/\overline{R}$.

With that said, there still remain a few open questions from the vibronic study of b4HPM[16] about the coupling of the excitonic states. One intriguing aspect addressed here is the small magnitude of the excitonic splitting observed in b4HPM relative to DPM. The splitting observed for both conformers is ≈132 cm^{-1} (see Table 3) and remarkably similar to the value of ≈123 cm^{-1} observed for DPM. The relative size of these splitting is to be contrasted with the ≈10-fold increase theoretically expected in the oscillator strengths of the electronic transitions in b4HPM relative to DPM.[16] As discussed in detail for DPM, a full treatment of the splitting within the traditional dipole−dipole coupling model necessarily requires taking into account geometric factors related to the overall structure and orientation factors that describe the localized TDMs. These are some of the issues we take up below.

A. S_0 and S_1 State Geometries. The rotational constants obtained from the theoretical predictions at the MP2/cc-pVTZ[31] level of theory for the two C_2 symmetric structures (labeled *dd* and *uu*) are shown beside the experimental values in Table 1. The optimized structures are shown in Figure 1. The calculated rotational parameters for both conformers are within 3% of the observed values. However, notice that the differences between the observed minus calculated parameters are larger than the changes in the observed constants for the two conformers. The 180° rotations of the OH groups that interconvert the *uu* and *dd* conformers are expected to have little impact on the rotational constants and, in fact, have been found in prior studies to be misleading regarding the actual OH orientation.[26] Thus, the assignments of the specific OH orientations of conformers A and B are not possible in this analysis. Although not performed in the current study, isotopic labeling of the hydroxyl proton may easily resolve this ambiguity.[26,32]

Table 4. Experimental Ground State Rotational Constants of the A and B Conformers of b4HPM[a]

		dd MP2/cc-pVTZ			*uu* MP2/cc-pVTZ		
conf. A	expt.[b]	opt	fit[c]	O−F[d]	opt	fit[c]	O−F[d]
A'' MHz	1569.78	1526.63	1569.8	+0.0	1516.91	1569.8	+0.0
B'' MHz	261.16	267.37	261.1	+0.1	267.90	261.1	+0.1
C'' MHz	250.15	255.80	250.9	−0.7	256.66	250.7	−0.5
α °		112.2	114.5	−2.3	112.2	114.8	−2.6
τ °		56.2	55.7	+0.5	56.9	55.0	+1.9
conf. B	expt.[b]	ppt	fit[c]	O−F[d]	opt	fit[c]	O−F[d]
A'' MHz	1571.89	1526.63	1571.9	+0.0	1516.91	1571.9	+0.0
B'' MHz	261.21	267.37	261.1	+0.1	267.90	261.2	+0.0
C'' MHz	249.96	255.80	250.7	−0.7	256.66	250.5	−0.5
α °		112.2	114.6	−2.4	112.2	114.8	−2.6
τ °		56.2	55.3	+0.9	56.9	55.4	+1.5

[a] The calculated values of the *uu* and *dd* isomers are compared with each conformer because the specific isomers are not distinguished. The rotational parameters for modified structures are also given where the two parameters, α and τ, were least squares fit to the experimental moments of inertia. [b] Experimental rotational constants obtained from MW measurements and rounded for clarity. [c] The fits were weighted according to the uncertainties propagated from the rotational constants. [d] Observed minus fit values for rotational constants and optimized (opt) minus fit values for α and τ.

Table 5. Comparison of the Experimental and Theoretical Results for the Two Lowest Excitonic States of b4HPM and DPM

	b4HPM				DPM	
	expt.		CIS[a,b]		expt.	CIS[a,b]
	A	B	*dd*	*uu*		
S_1 (B) eV	4.36	4.36	5.51	5.52	4.64	5.86
S_2 (A) eV	4.38	4.38	5.65	5.65	4.66	5.95
Δ_{12} cm^{-1c}	+132	+132	+1186	+1036	+123	+697
S_1 Osc. Str.			0.0618	0.0810		0.0058
S_2 Osc. Str.			0.0578	0.0461		0.0021
TDM *a*:	33(2)[d]:	27(2)[d]:	23:	10:	55(2)[d]:	35:
b:	20(2):	20(2):	36:	48:	17(3):	26:
c %	47(2)[e]	53(2)[e]	41	43	28(2)[f]	39
α °	114.7[g]	114.7[g]	114.0	114.3	114[g]	113.9
τ/°	55.4[g]	55.4[g]	45.1	45.3	57[g]	50.3

[a] Constrained to C_2 symmetry at the 6-311++G** level. The fully optimized geometry has C_1 symmetry. [b] Vertical excitation energies. [c] Exciton splitting between S_1 and S_2 states. [d] Uncertainties shown in parentheses refer to the last digits shown and are Type A, coverage factor $k = 1$ (1 std dev; ref 25). [e] Ratio determined from TDM of S_1 and vibronic band analysis from ref 16. [f] Ratio determined from TDM of S_1 from ref 15 and integrated vibronic band intensities from ref 14. [g] Estimates for the ground state geometry based on fits to MP2/cc-pVTZ geometry.

For the dipole−dipole model calculations discussed below, estimates of the structural parameters, τ and α, defined in Figure 1, are needed for model predictions. These are obtained from the least-squares fits to the experimental moments of inertia using the theoretical structures having all other structural parameters fixed. The fit results for all combinations are given in Table 4. The values for τ range from 55.0 to 55.7° and for α from 114.5 to 114.8°. In either case, the parameters are reliably determined to within a narrow range. Because the changes in the rotational constants of the S_1 states are small relative the S_0 values, similar values for α and τ are expected for the excited states. We also note the similarity to the respective values of 57.7 and 114.5° determined for DPM using this same level of theory.

B. Dipole Model Predictions of the Observed TDM Orientation. The relative magnitudes of the observed transition dipole moments (TDM) in the two exciton states may be obtained from results presented here and in the vibronic study.[16] As discussed above, the observed TDMs are delocalized and may be represented as relative projections along the *c*-, *a*-, and *b*-inertial axes. To obtain these projections, the relative oscillator strengths of the S_1 and S_2 states are first needed from the vibronic study.[16] These were determined from a multimode vibronic coupling analysis based on the Fulton and Gouterman[11,12] model. The S_1/S_2 ratio of transition strengths was reported to be 4:1 for conformer A and given the similarity of the vibronic band intensities,[16] this same ratio is expected for conformer B. From Tables 2 and 3, the relative TDM component magnitudes are determined within each exciton state: the S_2 states are pure *b*-type bands and the S_1 states are pure *a*-/*c*-type hybrid bands. The ratio of the oscillator strengths determines the relative scaling of the TDM magnitudes between the two exciton states. When taken together, the TDM magnitudes along the *a*:*b*:*c* principal axis are 33(2):20(2):47(2) % for conformer A and 27(2):20(2):53(2) % for B. These results are summarized in Table 5 along with the other electronic state properties of b4HPM and DPM.

For DPM,[15] a generalized set of algebraic equations were reported to calculate the delocalized TDM component amplitudes along the principal axes in terms of any arbitrary orientation of the localized TDM component amplitudes on the chromophores. The relative magnitudes (intensities) determined above are the square of these amplitudes. The equations are cast in terms of the flexible coordinates, τ and α, that define the structure in Figure 1 and ρ and β that describe the orientation of the localized TDM on each chromophore. The amplitude components are given by

$$x = \cos\rho \sin\tau \cos\beta - \cos\tau \sin\beta \tag{1a}$$

$$y = \left(\cos\tau \cos\frac{\alpha}{2}\cos\rho + \sin\rho \sin\frac{\alpha}{2}\right)\cos\beta + \sin\tau \cos\frac{\alpha}{2}\sin\beta \tag{1b}$$

$$z = \left(\cos\tau \sin\frac{\alpha}{2}\cos\rho - \sin\rho \cos\frac{\alpha}{2}\right)\cos\beta + \sin\tau \sin\frac{\alpha}{2}\sin\beta \tag{1c}$$

where *x*, *y*, and *z* correspond to the *c*-, *a*- (S_1), and *b*-axis (S_2) principal axis projections of the delocalized TDM amplitudes, respectively. The parameters, ρ and β, define the localized TDM orientation relative to the *p*-cresol subgroup, where ρ is the in-plane rotation angle referenced to zero for an orientation perpendicular to the C−CH_2 axis and β is the out-of-ring-plane angle. The structural parameters are held fixed at the average values of τ and α given in Table 4, and the solutions for ρ and β in eq 1 were obtained iteratively.

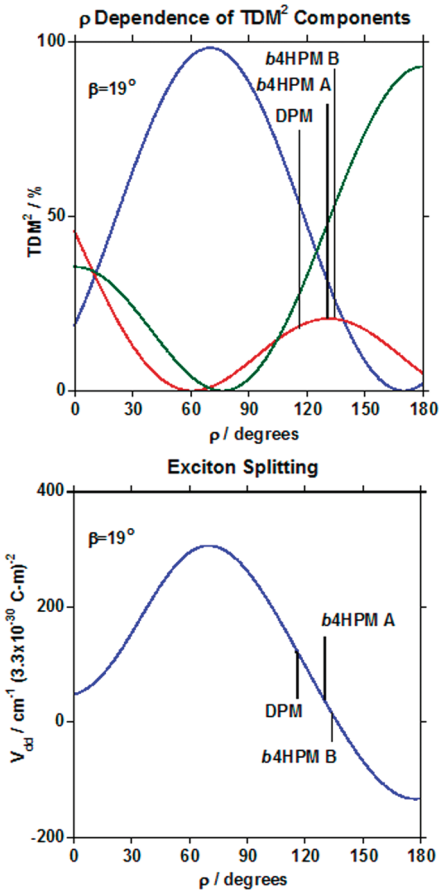

Figure 5. Squared components of the S_0-S_1 and S_0-S_2 TDMs (top) and the exciton splitting from the dipole−dipole coupling model (bottom) shown as a function of ρ for DPM and for conformers A and B of b4HPM.

It is first interesting to consider the case when the localized TDMs are in-plane and perpendicular to the C−CH_2 axes ($\rho = \beta = 0°$) as they are in *p*-cresol.[30] Eq 1 predict the *a*:*b*:*c* magnitude ratios of 9:23:68% for both conformers, which are in poor agreement with the observed TDM components of the S_1 states. Allowing for the in-plane rotation of the localized TDM, as observed for substituted benzenes,[33−35] the best fits to the experimental ratios of conformers A and B are for ρ = 21 and 15°, which gives 34:6:60% and 27:10:63%, respectively. In both cases, the S_2 band strengths are somewhat underestimated.

The observed orientations are predicted exactly when the out-of-plane terms in eq 1 are included in the fits. However, four unique solutions are possible since the orientations, not the directions and phases, of the TDMs are determined from the relative intensities. The solutions for (ρ,β) are: (14°,10°), (127°,72°), (**130°**,**19°**), (234°,26°) for A and (11°,7°), (138°,72°), (**134°**,**19°**), (231°,29°) for B. Four other equivalent pairs defined by $\rho \pm 180°$ for $-\beta$ designate the orientations for the chiral isomers of these conformers (see Figure 2).

It is impossible to determine which of the four sets discussed above is the correct one without further experimental data on isotopologues or detailed comparisons with ab initio results. However, a few aspects are worth noting to suggest the most likely candidates. As discussed in the earlier work,[16] the vibronic spectra of the two conformers are separated by only 24 cm^{-1} and the S_1 and S_2 origins have nearly identical excitonic splittings and relative oscillator strengths. Furthermore, from Table 2, the change in the TDM angles for the S_1 states is small, that is, ± 51(2)° for A versus ±54(2)° for B. This change is about half that for the *cis* (±66°) versus the *trans* (±74°) isomers of 2-hydroxynaphthalene.[26] Given these similarities, perhaps the most likely scenario would be the third set discussed above since the out-of-plane angles are the same and the in-plane angle changes by only 4°. The lack of a change in β might be expected because remote differences in the π orbitals between the *uu* to *dd* forms should have a minor effect on the out-of-plane overlap factors. It is also noteworthy that this solution has an out-of-plane angle remarkably close to that of DPM where (ρ,β) = 116°,20° was identified from detailed comparisons with ab initio results.[15] The square of the TDM components for β = 19° are shown for these three systems as a function of ρ in the top panel of Figure 5. The shifts in ρ by 14−18° relative to DPM are of similar magnitude to the changes observed in various substituted benzenes.[33−35]

C. Dipole Model Predictions of the Exciton Splitting. The localized TDM orientations allow some interpretation of the geometric factors affecting the excitonic splitting within the approximations of the dipole−dipole coupling model. The importance of these factors becomes apparent from ab initio results of the excitonic states. Geometry optimizations were performed at the Configuration Interaction Singles (CIS)[31] level where the best overall agreement with the TDM results was found for DPM. A summary of the observed and calculated excitonic state properties of b4HPM and DPM are given in Table 5. The excitonic splitting, Δ_{12}, in all cases, are overestimated by more than 5-fold in DPM and 8-fold for the isomers of b4HPM. However, as discussed in the vibronic study,[16] the observed splittings are necessarily smaller as a result of vibronic coupling. Of primary concern here is the small 7% increase observed in the relative excitonic splittings in b4HPM compared to that in DPM. As seen from Table 5, CIS theory predicts a slightly larger increase in Δ_{12} by ≈50%. However, these small differences are surprising considering the relative oscillator strengths predicted for the excitonic states are on average 10-fold larger in b4HPM than in DPM. Furthermore, a similar ratio of 0.064:0.0061 is predicted at the CIS/6-311++G** for the isolated chromophores, *p*-cresol and toluene, respectively.

The exciton splitting may also be estimated within the dipole−dipole coupling approximation using the expression given before[15]

$$V_{dd} = \frac{\mu_A \mu_B}{4\pi\varepsilon_0 R^3}(2\cos\theta_A \cos\theta_B + \sin\theta_A \sin\theta_B \cos\phi) \quad (2)$$

where μ is the magnitude of the localized TDM on each chromophore, R is the intermonomer separation, θ is the angle the localized TDM makes with the intermonomer axis, and φ is the dihedral angle between the localized TDMs. As shown for DPM,[15] eq 2 is expressed in terms of principal axis TDM components as

$$V_{dd} = -\frac{\mu_A \mu_B}{4\pi\varepsilon_0 R^3}(2y^2 - (1-y^2)(1-2z^2))$$
$$= -\frac{\mu_A \mu_B}{4\pi\varepsilon_0 R^3}(3y^2 + 2z^2 - 2y^2z^2 - 1) \quad (3)$$

The exciton splitting between the S_1 and S_2 states is $\Delta E = V_{dd}(S_2) - V_{dd}(S_1)$. Notice that V_{dd} is invariant to sign changes

in the y and z components and will be the same for any and all of the four (ρ,β) sets using eqs 1 and 3.

Of particular interest is the degree to which the orientation factors can account for the 10-fold ratio of oscillator strengths (see Table 5). The splittings calculated per unit TDM^2 from eq 3 are shown as a function of ρ for $\beta = 19°$ in the lower panel of Figure 5. For conformers A and B, the values of the splitting are $+40$ cm^{-1}/(3.3 $\times$ 10^{-30} C-m)^2 and $+17$ cm^{-1}/(3.3 $\times$ 10^{-30} C-m)^2, respectively (1 D = 3.3 $\times$ 10^{-30} C-m). Here, the 2-fold difference is exclusively a result of the 4° change in ρ. Likewise, for DPM, ΔE is $+126$ cm^{-1}/(3.3 $\times$ 10^{-30} C-m)^2. Therefore, the in-plane orientation factors in b4HPM have a significant impact on reducing the magnitude of the splitting relative to DPM by 4-fold on average. The reduction predicted for b4HPM occurs because the μ_{Local} orientations are more nearly perpendicular than in DPM. However, other factors are clearly at play to further reduce the excitonic interactions in b4HPM, including those discussed in the vibronic study that impact the degree of quenching ascribed to vibronic coupling of the ring and inter-ring modes.[16]

D. Beyond the Simple Models: S_1/S_2 State Perturbations and Mixing. Based on the TDM analysis given above, the rotationally resolved data suggest "textbook" cases of exciton coupling in this flexible bichromophore. However, several other aspects deserve mention that indicate the actual nature of the excited state levels are quite a bit more complicated than this simple exciton model would predict. As discussed in the vibronic paper,[16] the dispersed fluorescence spectra of b4HPM show clear signatures of vibronic coupling between the excitonic states. Enhanced S_2 origin emission to the ground state ring modes, 6a and 1, was strongly favored over the corresponding S_1 origin emission to these same levels. A quantitative measure of the coupling involving the two ring modes was obtained from fitting the vibronic band intensities to a multidimensional Fulton and Gouterman model.[11,12] The model predicted an S_2 state character composed of 60 % S^+ and 40 % S^- character, where S^+ and S^- are the respective zero-order states of S_2 and S_1 in the limit of no mixing. At a qualitative level, a similar enhancement of the S_2 versus S_1 emission to the ring modes was found in the dispersed emission spectra of DPM signifying vibronic coupling in this system as well.[14]

The vibronic studies of DPM[14] and b4HPM[16] also showed vibronic coupling of the S_2 origin with (nominally) S_1 inter-ring modes in close proximity. For these two molecules, the specific modes in near resonance with the S_2 states differ as a result of the frequency shifts associated with the increased reduced mass of the inter-ring modes in b4HPM. Consequently, coupling with the down-shifted ring-flapping pair, $R/\overline{R}$, occurs in b4HPM, while a similar coupling is not significant in DPM. In contrast, clear signatures of S_2 vibronic coupling with higher torsional quanta of $T/\overline{T}$ of S_1 were identified in DPM,[14] while the impact of this mode pair was much less significant in b4HPM.[16]

Of particular significance to these vibrational state specific enhancements is the complete lack of any rotational perturbations in the S_2 states of both conformers of b4HPM, despite the fact that the S_2 states in DPM and its isotopologues have rotational structure that is severely perturbed.[15] We can only speculate on the reason for their absence in b4HPM, because we have no firm knowledge of the nature of the interactions leading to the perturbations in DPM. The character of the vibronically coupled levels suggests a possible reason for these intrinsic differences. In DPM, all torsional minima on the ground and excitonic state surfaces are equivalent (see Figure 2 of ref 15). While details of the excited state surfaces are not known, other low energy pathways will likely exist for interconversion because of the high symmetry of the surface. As suggested previously,[15] the vibronic mixing of the S_2 origin with high torsional mode pairs of S_1 could result in tunneling that interconverts DPM between equivalent minima on a time scale competitive with the rotational motion and lead to rotational state perturbations from a Coriolis-type mechanism. For the *uu* and *dd* conformers of b4HPM, planar structures separate equivalent minima and, therefore, like the ground state in Figure 2, the direct tunneling pathways between equivalent minima on the excited state surfaces must pass through high torsional barriers. We also note that like the ground state surface, it is also likely that low barrier pathways exist on the excited state surfaces via the off-diagonal *ud* and *du* minima. In this case, the probability for tunneling will depend on the extent of wave function delocalization into the *ud* and *du* wells. For levels below the interconversion barriers, as expected for the zero-point levels of the S_2 origins, the delocalization will be small.[37] For these reasons, rotational state perturbations from Coriolis interactions would be diminished in b4HPM. Such changes relative to DPM may further explain the absence of any clear spectral signatures of $T/\overline{T}$ vibronic coupling in the dispersed fluorescence results.[16]

One final intriguing aspect of the S_2 states of b4HPM that remains unexplained is the 14200 MHz ($\approx$0.5 cm^{-1}) splitting observed for conformer B only. One possibility for the splitting might be torsional tunneling of the OH group(s) relative to the toluene-like frame(s). In phenol, the rotational lines of the $S_1 \leftarrow S_0$ origin spectrum are split by 56(4) MHz,[36] 55(4) MHz for the ^{18}O, and 59(4) MHz for the *para*-substituted deuterium isotopologues,[32] where most of this splitting is attributed to the torsional splitting on the ground state surface. However, the simultaneous OH torsional tunneling on the ground state surface shown in Figure 2 would convert the system between the *dd* and *uu* conformers or vice versa because the overall structure is chiral. As discussed above, the tunneling splitting between asymmetric minima on the surface is expected to be largely dampened when compared to that of phenol. Indeed, no splitting is observed for either ground state of b4HPM. A second possibility is that the S_2 origin undergoes a small inversion splitting associated with tunneling through a second lower energy barrier along the C_2 diagonal. A third and perhaps the most likely cause of the splitting would arise if the S_1 vibronic bands in B in close proximity to the S_2 origin are shifted slightly from their values in conformer A, with a new band gaining intensity through near resonant Herzberg–Teller vibronic coupling with the S_2 origin of B.[16] Indeed, as shown in the Supporting Information, the dispersed emission spectrum of the S_2(B) state is much more congested than that from the S_2(A) origin, indicating that there is a different vibrational makeup of the two bands responsible for the emission, consistent with this notion. Whatever the source, the difference in the rotational constants of the S_2 states of conformers A and B indicates a more than subtle change in the vibrationally averaged geometry associated with the S_2 surfaces. Further experimental characterization of the torsional state surfaces of *b*4HPM is currently underway using stimulated emission pumping population transfer measurements (SEP-PT)[38] to directly determine the barriers for interconversion between the *dd*, *ud*, and *uu* wells. These results will be reported elsewhere.[37] Such data will provide true measures of the quality of

predictions for further theoretical investigations of the excitonic interactions in this coupled system of flexible bichromophores.

V. CONCLUSIONS

The rotationally resolved UV spectra of two C_2 symmetric conformers and two exciton states of each conformer are fully assigned. The observed TDM orientations identify delocalized exciton states having TDM orientations in agreement with the classic example of strong excitonic coupling between two identical chromophores in close proximity. Both the structural data obtained from the rotational constants and band intensities obtained from the vibronic[16] and rovibronic spectra are decomposed in terms of the localized TDM vectors present on the two chromophores. The vectors were used in a dipole−dipole coupling model to assess the impact of the localized TDM orientations on the magnitude of the excitonic splitting. The orientation factors can only partially offset the 10-fold enhancement expected based on the predicted oscillator strengths when compared to diphenylmethane.

■ ASSOCIATED CONTENT

Supporting Information. Additional figures and data. This material is available free of charge via the Internet at http://pubs.acs.org.

■ AUTHOR INFORMATION

Corresponding Authors
*E-mail: david.plusquellic@nist.gov; zwier@purdue.edu.

■ ACKNOWLEDGMENT

C.P.R. and T.S.Z. gratefully acknowledge support from the Department of Energy Basic Energy Sciences, Division of Chemical Sciences under Grant No. DE-FG02-96ER14656. C.W.M. would like to thank the "Deutsche Akademie der Naturforscher Leopoldina" for a postdoctoral scholarship (Grant No. BMBF-LPD 9901/8-159 of the "Bundesministerium für Bildung und Forschung"). Certain equipment or software packages are identified in this paper in order to specify the experimental and computational procedures adequately. Such identification is not intended to imply endorsement by the National Institute of Standards and Technology nor is it intended to imply that the materials or equipment identified are necessarily the best available.

■ REFERENCES

(1) Baldo, M. A.; Thompson, M. E.; Forrest, S. R. *Nature* **2000**, *403*, 750.
(2) Bradley, M. S.; Tischler, J. R.; Bulovic, V. *Adv. Mater.* **2005**, *17*, 1881.
(3) Chan, J. M. W.; Tischler, J. R.; Kooi, S. E.; Bulovic, V.; Swager, T. M. *J. Am. Chem. Soc.* **2009**, *131*, 5659.
(4) Tischler, J. R.; Bradley, M. S.; Bulovic, V.; Song, J. H.; Nurmikko, A. *Phys. Rev. Lett.* **2005**, 95.
(5) Tischler, J. R.; Bradley, M. S.; Zhang, Q.; Atay, T.; Nurmikko, A.; Bulovic, V. *Org. Electron.* **2007**, *8*, 94.
(6) Muller, A.; Talbot, F.; Leutwyler, S. *J. Am. Chem. Soc.* **2002**, *124*, 14486.
(7) Muller, A.; Talbot, F.; Leutwyler, S. *J. Chem. Phys.* **2002**, *116*, 2836.
(8) Vandantzig, N. A.; Levy, D. H.; Vigo, C.; Piotrowiak, P. *J. Chem. Phys.* **1995**, *103*, 4894.
(9) Zwier, T. S. *J. Phys. Chem. A* **2006**, *110*, 4133.
(10) Ottiger, P.; Leutwyler, S.; Koppel, H. *J. Chem. Phys.* **2009**, *131*, 204308.
(11) Fulton, R. L.; Gouterman, M. *J. Chem. Phys.* **1961**, *35*, 1059.
(12) Fulton, R. L.; Gouterman, M. *J. Chem. Phys.* **1964**, *41*, 2280.
(13) Coffman, R.; McClure, D. S. *Can. J. Chem.* **1958**, *36*, 48.
(14) Pillsbury, N. R.; Stearns, J. A.; Muller, C. W.; Plusquellic, D. F.; Zwier, T. S. *J. Chem. Phys.* **2008**, *129*, 114301.
(15) Stearns, J. A.; Pillsbury, N. R.; Douglass, K. O.; Muller, C. W.; Zwier, T. S.; Plusquellic, D. F. *J. Chem. Phys.* **2008**, *129*, 224305.
(16) Rodrigo, C. P.; Muller, C. W.; Pillsbury, N. R.; James, W. H., III; Plusquellic, D. F.; Zwier, T. S. *J. Chem. Phys.* **2011**, *134*, 164312.
(17) Plusquellic, D. F.; Davis, S. R.; Jahanmir, F. *J. Chem. Phys.* **2001**, *115*, 225.
(18) Majewski, W.; Meerts, W. L. *J. Mol. Spectrosc.* **1984**, *104*, 271.
(19) Plusquellic, D. F.; Lavrich, R. J.; Petralli-Mallow, T.; Davis, S.; Korter, T. M.; Suenram, R. D. *Chem. Phys.* **2002**, *283*, 355.
(20) Riedle, E.; Ashworth, S. H.; Farrell, J. T.; Nesbitt, D. J. *Rev. Sci. Instrum.* **1994**, *65*, 42.
(21) Suenram, R. D.; Grabow, J. U.; Zuban, A.; Leonov, I. *Rev. Sci. Instrum.* **1999**, *70*, 2127.
(22) Grabow, J.-U; Stahl, W. *Z. Naturforsch.* **1990**, *A 45*, 1043. Grabow, J.-U.; Stahl, W.; Dreizler, H. *Rev. Sci. Instrum.* **1996**, *67*, 4072. Grabow, J.-U. private communication, 2003, see www.pci.uni-hannover.de/~lgpca/spectroscopy/ftmw/.
(23) Hageman, J. A.; Wehrens, R.; de Gelder, R.; Meerts, W. L.; Buydens, L. M. C. *J. Chem. Phys.* **2000**, *113*, 7955.
(24) Meerts, W. L.; Schmitt, M.; Groenenboom, G. C. *Can. J. Chem.* **2004**, *82*, 804.
(25) Taylor, B. N.; Kuyatt, C. E. *NIST Tech. Note*; 1994; Vol. *1297*. The publication may be downloaded from http://physics.nist.gov/Pubs/guidelines/contents.html.
(26) Johnson, J. R.; Jordan, K. D.; Plusquellic, D. F.; Pratt, D. W. *J. Chem. Phys.* **1990**, *93*, 2258.
(27) Majewski, W. A.; Pfanstiel, J. P.; Plusquellic, D. F.; Pratt, D. W. in *Laser Techniques in Chemistry*, Myers, A. B., Rizzo, T. R., Eds.; Wiley: New York, 1995; Vol. XXIII.
(28) Plusquellic, D. F. National Institute of Standards and Technology, jb95 software, v2.07.08; http://www.nist.gov/pml/div685/grp08/jb95.cfm.
(29) Plusquellic, D. F.; Suenram, R. D.; Mate, B.; Jensen, J. O.; Samuels, A. C. *J. Chem. Phys.* **2001**, *115*, 3057.
(30) Myszkiewicz, G.; Meerts, W. L.; Ratzer, C.; Schmitt, M. *J. Chem. Phys.* **2005**, *123*, 044304.
(31) Frisch, M. J., Trucks, G. W.; Schlegel, H. B.; Scuseria, G. E.; Robb, M. A.; Cheeseman, J. R.; Scalmani, G.; Barone, V.; Mennucci, B.; Petersson, G. A.; Nakatsuji, H.; Caricato, M.; Li, X.; Hratchian, H. P.; Izmaylov, A. F.; Bloino, J.; Zheng, G.; Sonnenberg, J. L.; Hada, M.; Ehara, M.; Toyota, K.; Fukuda, R.; Hasegawa, J.; Ishida, M.; Nakajima, T.; Honda, Y.; Kitao, O.; Nakai, H.; Vreven, T.; J. A. Montgomery, J.; Peralta, J. E.; Ogliaro, F.; Bearpark, M.; Heyd, J. J.; Brothers, E.; Kudin, K. N.; Staroverov, V. N.; Kobayashi, R.; Normand, J.; Raghavachari, K.; Rendell, A.; Burant, J. C.; Iyengar, S. S.; Tomasi, J.; Cossi, M.; Rega, N.; Millam, J. M.; Klene, M.; Knox, J. E.; Cross, J. B.; Bakken, V.; Adamo, C.; Jaramillo, J.; Gomperts, R.; Stratmann, R. E.; Yazyev, O.; Austin, A. J.; Cammi, R.; Pomelli, C.; Ochterski, J. W.; Martin, R. L.; Morokuma, K.; Zakrzewski, V. G.; Voth, G. A.; Salvador, P.; Dannenberg, J. J.; Dapprich, S.; Daniels, A. D.; Farkas, Ö.; Foresman, J. B.; Ortiz, J. V.; Cioslowski, J.; Fox, D. J. *Gaussian 03*, Revision A.1; Gaussian, Inc.: Wallingford, CT, 2009.
(32) Ratzer, C.; Küpper, J.; Spangenberg, D.; Schmitt, M. *Chem. Phys.* **2002**, *283*, 153.
(33) Borst, D. R.; Joireman, P. W.; Pratt, D. W.; Robertson, E. G.; Simons, J. P. *J. Chem. Phys.* **2002**, *116*, 7057.
(34) Joireman, P. W.; Kroemer, R. T.; Pratt, D. W.; Simons, J. P. *J. Chem. Phys.* **1996**, *105*, 6075.

(35) Kroemer, R. T.; Liedl, K. R.; Dickinson, J. A.; Robertson, E. G.; Simons, J. P.; Borst, D. R.; Pratt, D. W. *J. Am. Chem. Soc.* **1998**, *120*, 12573.
(36) Berden, F.; Meerts, W. L.; Schmitt, M.; Kleinermanns, K. *J. Chem. Phys.* **1996**, *104*, 972.
(37) Rodrigo, C. P.; Muller, C. W.; Plusquellic, D. F.; Zwier, T. S. 2011, manuscript in preparation.
(38) Pillsbury, N. R.; Muller, C. W.; Zwier, T. S. *J. Phys. Chem. A* **2009**, *113* (17), 5013.

■ NOTE ADDED AFTER ASAP PUBLICATION

This article post ASAP on June 3, 2011. References 27 and 28 have been revised. The correct version posted on June 10, 2011.